

**The Response of Structures with Uncertain Joint Properties:
A Component Modal Approach**

A. Stenti, B.R. Mace and P. Sas

ISVR Technical Memorandum 906

April 2003



SCIENTIFIC PUBLICATIONS BY THE ISVR

Technical Reports are published to promote timely dissemination of research results by ISVR personnel. This medium permits more detailed presentation than is usually acceptable for scientific journals. Responsibility for both the content and any opinions expressed rests entirely with the author(s).

Technical Memoranda are produced to enable the early or preliminary release of information by ISVR personnel where such release is deemed to be appropriate. Information contained in these memoranda may be incomplete, or form part of a continuing programme; this should be borne in mind when using or quoting from these documents.

Contract Reports are produced to record the results of scientific work carried out for sponsors, under contract. The ISVR treats these reports as confidential to sponsors and does not make them available for general circulation. Individual sponsors may, however, authorize subsequent release of the material.

COPYRIGHT NOTICE

(c) ISVR University of Southampton All rights reserved.

ISVR authorises you to view and download the Materials at this Web site ("Site") only for your personal, non-commercial use. This authorization is not a transfer of title in the Materials and copies of the Materials and is subject to the following restrictions: 1) you must retain, on all copies of the Materials downloaded, all copyright and other proprietary notices contained in the Materials; 2) you may not modify the Materials in any way or reproduce or publicly display, perform, or distribute or otherwise use them for any public or commercial purpose; and 3) you must not transfer the Materials to any other person unless you give them notice of, and they agree to accept, the obligations arising under these terms and conditions of use. You agree to abide by all additional restrictions displayed on the Site as it may be updated from time to time. This Site, including all Materials, is protected by worldwide copyright laws and treaty provisions. You agree to comply with all copyright laws worldwide in your use of this Site and to prevent any unauthorised copying of the Materials.

UNIVERSITY OF SOUTHAMPTON
INSTITUTE OF SOUND AND VIBRATION RESEARCH
DYNAMICS GROUP

**The Response of Structures with Uncertain
Joint Properties: A Component Modal Approach**

by

A. Stenti, B.R. Mace and P. Sas

ISVR Technical Memorandum No: 906

April 2003

Authorised for issue by
Professor M.J. Brennan
Group Chairman

Abstract

Built-up structures include joints such as spot welds, bolted joints, gaskets etc., whose physical properties, e.g. stiffness, thickness, damping, often vary substantially from one structure to another. Uncertainties in these physical properties lead to significant uncertainties in the dynamic behaviour of the structure, and there is therefore an interest in predicting the statistics of the response given the statistics of the joint properties.

There are two main issues. The first involves quantifying the statistics of the joint properties, which, for line junctions, potentially includes spatial correlation. The second issue is the development of a computationally efficient numeric procedure to calculate the response statistics. This report addresses the second issue. Component mode synthesis (CMS) is used to describe the behaviour of the connected components. This approach reduces the size of a numerical model, while the uncertainties are then associated with the properties of the structure at the interface. Various methods are then considered by which the response statistics can be estimated. Numerical examples are presented.

Contents

1.	Introduction.....	4
2.	Component Mode Synthesis.....	6
	2.1 Introduction	
	2.2 Background Theory	
	2.3 Fixed-Interface CMS	
3.	A Numerical Example: Deterministic Properties.....	15
	3.1 Model Description	
	3.2 Full Finite Element Analysis	
	3.3 CMS – Finite Element Analysis	
4.	Uncertainty and Variability.....	26
5.	A Numerical Example: Uncertain Properties.....	28
	5.1 Model Description	
	5.2 Monte Carlo Simulation	
6.	Future Work: Perturbational Methods.....	37
7.	Concluding Remarks.....	40
8.	Acknowledgements.....	41
9.	References.....	42

1. Introduction

Higher frequency noise and vibration modelling in built-up structures such as cars, aircraft, manufactured products etc. is an increasing problem in modern industry. Audio-frequency noise and vibration performance is important, and hence the engineer needs to design for low-noise products. One problem faced by the engineer, however, is that mass-produced products are never exactly the same because of manufacturing variability and so on. Thus some of the structures are noisier than others. The engineer needs to take into account uncertainties and variability in the properties when designing for noise and vibration behaviour, to eliminate, as far as is practical, the occurrence of structure, which are unacceptably noisy or vibration-prone.

The long-term aim of this research is the development of engineering tools for numerical modelling, product refinement and Virtual Prototyping, particularly where product variability and data uncertainty is a major problem. Specific attention will be focussed on the behaviour of built-up structures where there is uncertainty and variability in the properties of the joints that connect the various component parts. Uncertainty and variability in the properties of different physical realisations of a system produce variations in their responses and therefore differences in the noise and vibration behaviour of the items. These differences become larger at higher frequencies. Thus the engineer is interested in not only the ‘baseline’ response prediction, but also estimates of the statistics or spread of the responses of different realisations of the structure.

One existing technique for vibration modelling involves a finite element analysis (FEA) of the structure. This is appropriate if the properties are known exactly and if the frequency is low. An alternative approach for high frequencies is statistical energy analysis (SEA) [1], which assumes wide random variations in the properties of the structures. In the ‘mid-frequency’ range, which is the subject of this report, a statistical approach is required, but the properties do not vary as widely as assumed in SEA.

A number of statistical approaches have been developed to allow for uncertainties in the parameters of a structure to be included in a numerical analysis [2]. Parameter uncertainties can be incorporated in deterministic models, often by finding perturbational relations between parameters and response quantities [3,4,5,6]. Also important are stochastic FE methods [7,8], where the continuous physical properties of the structure vary statistically and are meshed in a manner analogous to that used to discretise the structure itself.

Monte Carlo simulations can also be used, by repeating an exact calculation many times with different sets of parameters. These approaches can be prohibitively expensive, and are typically applied to cases of modest uncertainty at low frequencies.

In the mid-frequency range the wavelength of interest is such that large FE models are typically needed for the solution. Even a single deterministic solution of a large FE model is

a computationally expensive task. When uncertainties are included in the structure repeating an exact calculation many times for evaluating the response statistics, e.g. as in the case of a Monte Carlo simulation, becomes impractical. Developing techniques that reduce the order of large FE models and allows the introduction of uncertainties in the structure in a fast and robust way is a major need.

In this report a sub-structuring technique, Component Mode Synthesis (CMS) [9] is preferred. In CMS the structure is divided into substructures, each modelled individually, and the uncertainties introduced locally in the substructures. The substructures are then assembled to produce a much smaller model of the structure as a whole. Several advantages of this method are shown via a straightforward numerical example.

A comparison is made between a full FEA and a CMS-FEA. The response statistics are evaluated via a Monte Carlo simulation. The CMS-FEA is computationally much cheaper while a high accuracy is in general retained. However, a direct Monte Carlo simulation, resolving for the complete structure (FEA) or locally for each substructure (CMS-FEA) is still a computationally expensive task. The development of alternative methods such as probabilistic dynamic synthesis [10], perturbational methods, etc, to substantially reduce computational cost is therefore needed.

In chapter 2 the CMS method is introduced. In chapter 3 full FEA and CMS-FEA of an example structure are compared. Advantages deriving from the use of CMS are shown. At this stage the model is still deterministic. In chapter 4 the need to introduce uncertainties in a structure and to consider variability in its responses are explained. In chapter 5 uncertainties are introduced in the properties of the joint of the example structure. A direct Monte Carlo simulation is performed to evaluate the response statistics. Full FEA and CMS-FEA are compared.

A direct Monte Carlo simulation is still an expensive computational task. In chapter 6 a perturbational method is introduced, for which the response statistics are evaluated at an insignificant cost. Results and comparisons between the various methods presented (FEA vs. CMS-FEA via a direct Monte Carlo simulation and a perturbational method) are the long-term aim of this research.

2. Component Mode Synthesis

2.1. Introduction

Component mode synthesis is, in essence, a method for reducing the order of large finite element models. Large models are typical of complex built-up structures, such as airplanes, cars, helicopters etc.

The method has fundamentally three steps. In the first step the structure is divided into substructures. Then a reduced-order component-mode model represents each substructure. Finally the component models are coupled to form a reduced-order system model.

While there are many methods for reducing the order of large finite element models, CMS is, in most cases, the most systematic and efficient procedure for developing a satisfactory reduced-order model. Among the first to contribute to this method are Gladwell [11], Hurty [12], Craig and Bampton [13], Goldman [14], Hou [15], Bajan et al. [16], MacNeal [17], and Benfield and Hruda [18].

The CMS method has several advantages. By reducing the order of large FE models in a manner similar to a general mode substitution criterion it addresses principally the need to reduce computational cost. Often components made independently have properties that are also statistically independent and the CMS, being a sub structuring technique, allows each substructure to be treated almost independently. This gives the analyst a wide range of possibilities, such as modelling each substructure in different ways, e.g. via a FE model, a statistical energy representation (SEA), using analytical models, using experimental data such as frequency response functions, etc. The independent ways in which the substructures can be treated also gives advantages in terms of minimising the re-analysis time when localised modifications are investigated (i.e. the re-analysis has to be run locally rather than globally).

The aim of this report is to develop a robust and fast technique for including uncertainties in the joints of built-up structures. It is clear how CMS can be useful when, in order to evaluate the response statistics of interest, instead of running a Monte Carlo simulation on the full structure, the uncertainties can be introduced locally in a substructure rather than globally in the structure. Only a local analysis has to be performed, in order to retrieve the same statistics, reducing enormously the computing time.

2.2. Background Theory

The first step in the analysis is to divide the complete structure into a number of substructures. A substructure is typically connected to one or more adjacent substructures by interfaces. The substructure nodal coordinates are partitioned into interior coordinates (i.e. not shared with adjacent substructures), and interface or coupling coordinates (i.e. shared with adjacent substructures).

Figure (1) illustrates a simple cantilever beam that is divided into three substructures; the middle one is a typical substructure with interfaces. The coordinate sets C and I represents the coupling and interior coordinates respectively.

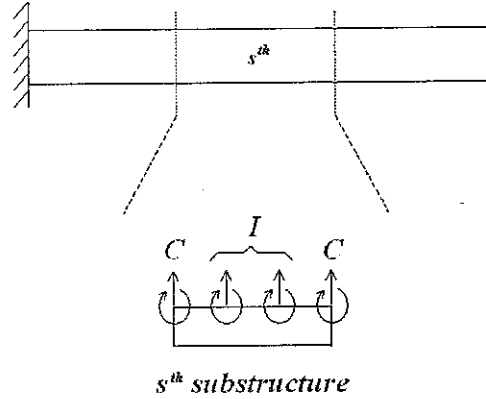


Figure (1): a typical substructure with interfaces.

The equation of motion of the s^{th} undamped substructure in its FE representation may be written as

$$[M]^s \{\ddot{x}\}^s + [K]^s \{x\}^s = \{f\}^s \quad (1.1)$$

where $[M]^s$, $[K]^s$, $\{x\}^s$ and $\{f\}^s$ are the mass matrix, stiffness matrix, displacement vector, and vector of externally applied forces, for the s^{th} substructure respectively. Different sets of coordinates can be used to partition $\{x\}^s$. A full description is given in reference [9, 11-19], and in section 2.2 for a specific CMS method.

Once the substructure procedure is established, the next step in the analysis is the definition of a set (or sets) of component modes, followed by the coupling of component models to form a reduced-order system model.

In CMS, the substructure's physical displacement coordinates $\{x\}^s$ are typically represented in terms of component-generalised coordinates $\{q\}^s$ by the Ritz coordinate transformation

$$\{x\}^s = [\psi]^s \{q\}^s \quad (1.2)$$

where the component mode matrix $[\psi]^s$ is a matrix of pre-selected component modes. The term component mode is used to signify a class of assumed modes that are used as basis vectors in describing the displacement of nodes within a substructure. Component normal modes (eigenvectors) are one class of assumed modes [9]. A large variety of component modes can be involved in a component mode analysis, to form the matrix $[\psi]^s$. Such component modes are typically constraint modes, rigid body modes, attachment modes, inertia relief modes, normal modes (both fixed-interface and free-interface), etc, for which a full description is found in references [9, 11-19].

Two decisions must be made in forming the component mode matrix $[\psi]^s$: first, the types of component modes to include, and second, the number of modes of each type that has to be retained in the analysis. There are various methods of component mode synthesis each related to the choice of component modes to be included in $[\psi]^s$. It is of vital importance to select a good transformation matrix.

In [20] Noor and Peters list the following criteria for selection of the vectors to form the transformation matrix $[\psi]^s$:

“Linear independence and completeness;

Low computational expense in their generation, and simplicity of automatic selection of their number;

Good approximation properties, in the sense of high accuracy of the solution obtained using these vectors;

Simplicity of obtaining the system response characteristics of interest using these vectors.”

A combination of constraint modes (which includes rigid-body modes) and fixed interface normal modes fulfils all of the above criteria. A description of the fixed-interface approach is given in section 2.2. Methods that employ free-interface normal modes, together with their static corrections (interface attachment modes, etc), are in general much more difficult to implement than fixed interface. In general, if any reduced set of component normal modes or any other set of assumed modes is used without including a complete set of either interface constraint modes or interface attachment modes, the component mode set is not statically complete, so the first criterion is violated. We can therefore recognize three main variants of CMS methods, each related to the specific set of component modes selected to form the transformation matrix $[\psi]^s$: fixed-interface methods, free interface methods and hybrid methods (a combination of fixed-interface and free-interface methods). The fixed-interface methods tend to have improved convergence characteristics. In case of FE models, the Craig-Bampton fixed-interface method [13] is frequently used. Free interface methods are more useful when considering experimentally derived component modes.

Once the component-mode matrix $[\psi]^s$ is established, the transformation (1.2) is used together with the equation of motion of the substructure (1.1) to form the component modal model. In order to reduce the order of the model, a reduced form of the matrix $[\psi]^s$ is considered. Here a fundamental assumption is made which states that only a few modes contribute to the response of the complete structure. Then, only a certain number of modes are retained in $[\psi]^s$ leading to a reduced order model. The reduced order model is in the form

$$[\bar{M}]^s \{\ddot{q}\}^s + [\bar{K}]^s \{q\}^s = \{\bar{f}\}^s \quad (1.3)$$

where the system matrices are

$$[\bar{M}]^s = [\psi]^s{}^T [M]^s [\psi]^s, \quad [\bar{K}]^s = [\psi]^s{}^T [K]^s [\psi]^s, \quad \{\bar{f}\}^s = [\psi]^s{}^T \{f\}^s \quad (1.4)$$

The last step of the analysis is the synthesis process, where the local finite element models of each substructure are then coupled together by enforcing continuity. There are several ways in which the compatibility equations can be applied to the system. In [13], Craig and Chang introduce a generalized procedure for coupling component models to form system equation of motion. In general, constraint equations in terms of component coordinates can be written as

$$[C][q] = 0 \quad (1.5)$$

In [9], the synthesis of the equations of motion is based on Lagrange's equation of motion with undetermined multipliers. A simpler way is used in [6], where a matrix transformation takes into account the coupling between the different component coordinates, namely

$$\{q\} = [D]\{p\} \quad (1.6)$$

where $\{p\}$ represents the coupled component modal coordinates. Other techniques are possible, all leading to a reduced order of the complete system equation of motion

$$[M]\{\ddot{p}\} + [K]\{p\} = \{f\} \quad (1.7)$$

where the global mass and stiffness matrices of the complete structure are in general sparse, and expressed in terms of global coupled component modal coordinates.

2.3. Fixed-Interface CMS

Component coupling is straightforward if the component-mode matrix $[\psi]^s$ consists of only interface constraint modes and fixed-interface normal modes. Such a choice of $[\psi]^s$ was first introduced by Hurty [11] and then simplified by Craig and Bampton. [13].

Following [6], a simple way of describing how the method works is presented. A distinction is made between three sets of coordinates used to describe the response of the structure: nodal degrees of freedom $\{x\}$, uncoupled component modal degrees of freedom $\{q\}$, coupled component modal degrees of freedom $\{p\}$. The last are similar to $\{q\}$ except for the fact that they take into account the compatibility equations between the boundary degrees of freedom of all the substructures.

The nodal degrees of freedom $\{x\}$ represent the physical displacement of the complete structure. The vector is partitioned into the degrees of freedom associated with each subsystem so that

$$\{x\} = \begin{Bmatrix} x^1 \\ x^2 \\ \vdots \\ x^N \end{Bmatrix} \quad (2.1)$$

where N is the number of substructures in which the structure has been divided, and each element of $\{x\}$ is a column vector of nodal degree of freedom for the relative substructure. Each sub-vector of $\{x\}$ is further partitioned into interior and coupling degrees of freedom. The degrees of freedom associated with the s^{th} subsystem are then given by

$$\{x\}^s = \begin{Bmatrix} x_i \\ x_c \end{Bmatrix}^s \quad (2.2)$$

where the subscripts i and c refer to interior and coupling degrees of freedom respectively. $\{x_i\}^s$ can be any set of specified generalized coordinates describing the deformation of the interior of the substructure. The coordinate $\{x_c\}^s$ represents physical displacements of coupling degrees of freedom. The coupling degrees of freedom in a given substructure are later related to those in the adjacent substructures through the use of a number of constraint equations. The above partition leads to

$$\begin{bmatrix} M_{ii}^x & M_{ic}^x \\ M_{ci}^x & M_{cc}^x \end{bmatrix}^s \begin{Bmatrix} \ddot{x}_i \\ \ddot{x}_c \end{Bmatrix}^s + \begin{bmatrix} K_{ii}^x & K_{ic}^x \\ K_{ci}^x & K_{cc}^x \end{bmatrix}^s \begin{Bmatrix} \ddot{x}_i \\ \ddot{x}_c \end{Bmatrix}^s = \begin{Bmatrix} f_i^x \\ f_c^x \end{Bmatrix}^s \quad (2.3)$$

where $[M_{ii}^x]^s$, $[K_{ii}^x]^s$, $[M_{ic}^x]^s \dots \{f_i^x\}^s$, $\{f_b^x\}^s$, are the appropriate partition of the substructure matrices and the force vector of the externally applied forces respectively, expressed in nodal degrees of freedom $\{x\}$. If we have n^x nodal coordinates, n_i^x interior coordinates and n_c^x coupling coordinates, with $n^x = n_i^x + n_c^x$, the substructure sub-matrices will be of dimensions $[M_{ii}^x]^s_{n_i^x \times n_i^x}$; $[K_{ii}^x]^s_{n_i^x \times n_i^x}$; $[M_{ic}^x]^s_{n_i^x \times n_c^x} \dots \{f_i^x\}^s_{n_i^x \times 1}$, $\{f_c^x\}^s_{n_c^x \times 1}$ respectively.

The undamped equations of motion for the uncoupled complete structure then take the form

$$[M^x]\{\ddot{x}\} + [K^x]\{x\} = \{f^x\} \quad (2.4)$$

where the matrices $[M^x]$ and $[K^x]$, following the partition (2.2), are block diagonal with each of their sub matrices in the form (2.3). The superscript indicates again the coordinate system in which they are defined.

A local modal analysis of each substructure is then performed with the coupling degrees of freedom associated with each substructure being fully constrained. A subset of the local modes is generally considered. The nodal degrees of freedom are related to the uncoupled component modal degrees of freedom by the transformation matrix

$$\{x\} = [\psi]\{q\} \quad (2.5)$$

where $[\psi]$ takes the form of a block diagonal matrix of dimension n^x by n^q ; where n^x is the number of nodal coordinates and n^q is the number of uncoupled component modal coordinates. The s^{th} sub matrix on the diagonal of $[\psi]$ is given by

$$[\psi]^s = \begin{bmatrix} \phi_{N_r} & \phi_c \\ O & I \end{bmatrix}^s \quad (2.6)$$

$$\{x\}^s = \begin{Bmatrix} x_i \\ x_b \end{Bmatrix}^s = \begin{bmatrix} \phi_{N_r} & \phi_c \\ O & I \end{bmatrix}^s \begin{Bmatrix} q_{N_r} \\ x_c \end{Bmatrix}^s \quad (2.7)$$

where $[\phi_c]$ represents the vector of constraint modes, N_r , the number of retained fixed interface normal modes and $[\phi_{N_r}]$ the vector of retained fixed interface normal modes. Constraint modes are defined as the mode shapes of interior degrees of freedom due to a successive unit displacement of coupling degrees of freedom, all other coupling degrees of freedom being totally constrained. To determine the constraint modes the forces at all interior degree of freedoms are set equal to zero. Equation (2.3) gives

$$\{0\} = [K_{ic}^x]^s \{x_c\}^s + [K_{ii}^x]^s \{x_i\}^s \quad (2.8)$$

or

$$\{x_i\}^s = -[K_{ii}^x]^{s-1} [K_{ic}^x] \{x_c\}^s = [\phi_c] \{x_c\}^s \quad (2.9)$$

The substructure normal modes are defined as the normal modes of the substructure with totally constrained coupling degrees of freedom. These are obtained from the equations

$$\{x_i\}^s = \{\phi_i\} e^{i\omega t}, \quad \omega^2 [M_{ii}^x] \{\phi_i\} = [K_{ii}^x] \{\phi_i\} \quad (2.10)$$

The eigenvectors of equation (2.10) are the normal modes of the constrained substructure. These eigenvectors form the respective columns of the matrix $[\phi_{Nr}]^s$. The mode shapes are assumed to be mass normalised so that

$$[\phi_{Nr}]^{sT} [K_{ii}^x] [\phi_{Nr}]^s = [\text{diag}(\omega_{local}^2)] \quad (2.11)$$

and

$$[\phi_{Nr}]^{sT} [M_{ii}^x] [\phi_{Nr}]^s = I \quad (2.12)$$

The transformation (2.5) together with the uncoupled system equation of motion (2.4) gives the uncoupled component modal equation of motion for the complete structure

$$[M^q] \{\ddot{q}\} + [K^q] \{q\} = \{f^q\} \quad (2.13)$$

where the global mass and stiffness matrices and the forcing vector are respectively in the form

$$[M^q] = [\psi]^T [M^x] [\psi], \quad [K^q] = [\psi]^T [K^x] [\psi], \quad \{f^q\} = [\psi]^T \{f^x\} \quad (2.14)$$

where $[M^q]$, and $[K^q]$ are block diagonal, with their s^{th} sub-matrices given respectively by

$$[M^q]^s = [\psi]^sT [M^q]^s [\psi]^s, \quad [K^q]^s = [\psi]^s [K^q]^s [\psi]^s \quad (2.15)$$

Partitioning these sub-matrices into normal and constraint mode terms and noting that the fixed interface normal modes are mass and stiffness orthogonal gives

$$[M^q]^s = \begin{bmatrix} I & M_{ic}^q \\ M_{ci}^q & M_{cc}^q \end{bmatrix}^s, \quad [K^q]^s = \begin{bmatrix} \omega_{local}^2 & O \\ O & K_{cc}^q \end{bmatrix}^s \quad (2.16)$$

The normal modes are stiffness orthogonal with respect to the constraint modes whilst the constraint modes are neither mass nor stiffness orthogonal. The sub-matrices $[M_{cc}^q]^s$, $[M_{ci}^q]^s$, $[M_{ic}^q]^s$ and $[K_{cc}^q]^s$ are generally full, and $[M_{ci}^q]^s = [M_{ic}^q]^s$.

The local FE models are then coupled by enforcing continuity between the various coupling degrees of freedom. The uncoupled component modal coordinates $\{q\}$ can be related to a set of coupled component modal coordinates $\{p\}$, using the transformation matrix $[B]$, so that

$$\{q\} = [B]\{p\} \quad (2.17)$$

whilst the uncoupled component modal coordinates of substructure s , $\{q\}^s$, are related to the set of coupled component modal coordinates by the appropriate partition of $[B]$, i.e.,

$$\{q\}^s = [B]^s \{p\} \quad (2.18)$$

The undamped global equations of motion are then given by:

$$[M^p]\{\ddot{p}\} + [K^p]\{p\} = \{f^p\} \quad (2.19)$$

where the global mass and stiffness matrices and the global force vector are given by

$$[M^p] = [B]^T [M^q] [B], \quad [K^p] = [B]^T [K^q] [B], \quad \{f^p\} = [B]^T \{f^q\} \quad (2.20)$$

Due to the block diagonal nature of the matrices in equation (2.19), the global mass, stiffness and force matrices can be written in the form

$$[M^p] = \begin{bmatrix} I & O & \cdots & M_{ic,1}^q B^1 \\ O & I & \cdots & M_{ic,2}^q B^2 \\ \vdots & \vdots & \ddots & \vdots \\ B^{1T} M_{ci,1}^q & B^{2T} M_{ci,2}^q & \cdots & \sum_s B^{sT} M_{cc,s}^q B^{sT} \end{bmatrix} \quad (2.21)$$

$$[K^p] = \begin{bmatrix} \omega_{local,1}^2 & O & \cdots & O \\ O & \omega_{local,2}^2 & \cdots & O \\ \vdots & \vdots & \ddots & O \\ O & O & \cdots & \sum_s B^{sT} K_{cc,s}^q B^{sT} \end{bmatrix} \quad (2.22)$$

$$\{f^p\} = \begin{bmatrix} f_{i,1}^q \\ f_{i,2}^q \\ \vdots \\ \sum_s B^{sT} f_{c,s}^q \end{bmatrix} \quad (2.23)$$

In (2.19) $[M^p]$, $[K^p]$ and $\{f^p\}$ have dimensions $n^p \times n^p$, $n^p \times n^p$, and $n^p \times 1$, respectively, where n^p is the number of coupled component modal coordinates. Since in the analysis only a subset of modes for each substructure is considered, the resulting assembled matrices for the complete structure are of order n^p , which is substantially less than the number of nodal degrees of freedom n^x in a full FE. The order of the structure is therefore substantially reduced.

3. A Numerical Example: Deterministic Properties

3.1. Model Description

In this and the following sections a full FEA and a CMS-FEA are performed on a case-study example. The aim is to show the advantages of using a CMS-FEA in terms of computing time saving while high accuracy in the results is generally retained. The interest of this research is to show the advantages of using such a method when including uncertainties in the structure especially in the property of the joints. Therefore a case-study example consisting of three plates joined together is considered. The plate of small dimensions characterise the joint connection. Each plate is clamped at one edge, with two edges being free, as shown in Figure (2).

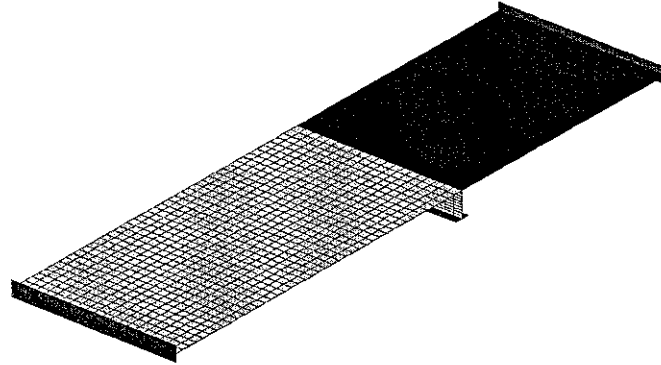


Figure (2): the model consisting of three plates joined together.

The dimensions of the structure are:

first plate:	<i>length</i>	=	1	[m]
	<i>width</i>	=	0.5	[m]
	<i>thickness</i>	=	0.05	[m]
second plate:	<i>length</i>	=	$\sqrt{2}$	[m]
	<i>width</i>	=	0.5	[m]
	<i>thickness</i>	=	0.05	[m]
third plate:	<i>length</i>	=	0.1	[m]
	<i>width</i>	=	0.5	[m]
	<i>thickness</i>	=	0.05	[m]

All three plates are of the same homogeneous, isotropic, material; namely steel, whose properties are:

$$\begin{array}{llll} \text{Young's modulus:} & E & = & 210 \quad [GPa] \\ \text{Density:} & \rho & = & 7850 \quad [Kg/m^3] \\ \text{Poisson's ratio:} & \nu & = & 0.3 \end{array}$$

The material behaviour is assumed to be elastic.

The *MATLAB Structural Dynamic Toolbox (STD)* was used to develop the FE model. The FE model consists of 1848 nodes and 1744 finite elements. For each node all the degrees of freedom are retained. Type Quad4 elements have been used with some drilling capabilities, according to the definition given in the *MATLAB STD* manual. The resulting model has a total of 11088 degrees of freedom

3.2. Full Finite Element Analysis

In the first step a full FEA is performed. The transfer mobility between the excitation and the observation points chosen as in Figure (3) is then evaluated. The excitation/observation points are chosen to lie away from the plane of symmetry (i.e. xz) of the structure. The eigenproblem is solved for the undamped structure. Proportional damping of 1% is then added for the evaluation of the frequency response functions (FRFs).

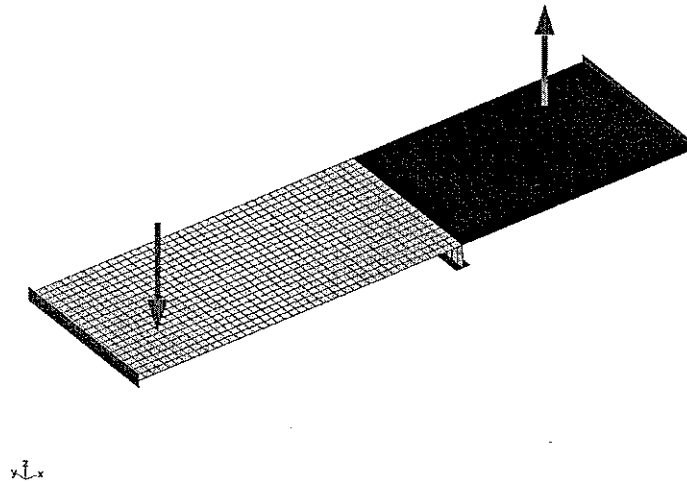


Figure (3): excitation/observation points.

The full FEA took 420 seconds to run (on a *Pentium 4, 1.7GHz*), and 300 modes found up to 16000 Hz. Figure (4) and (5) show the mobility up to 10000 Hz and in the low frequency range respectively. The frequency resolution is 1 Hz.

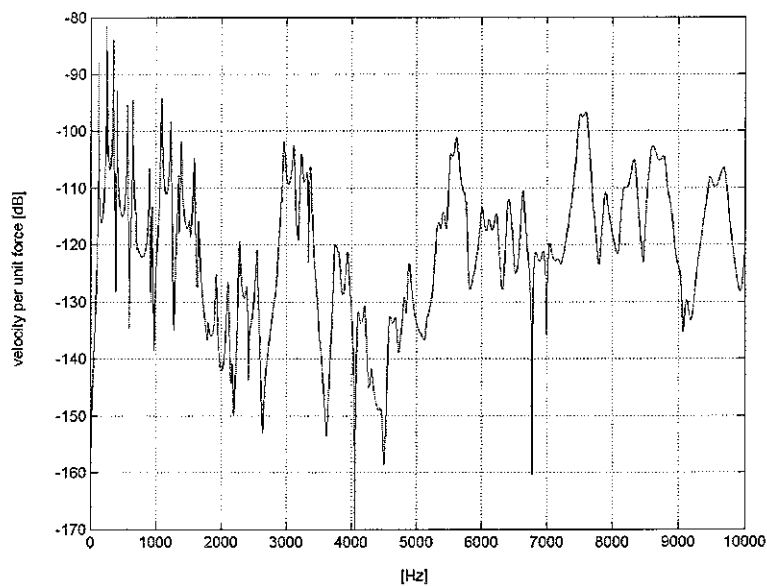


Figure (4): 0-10000 Hz plot of mobility between the chosen e/o points.

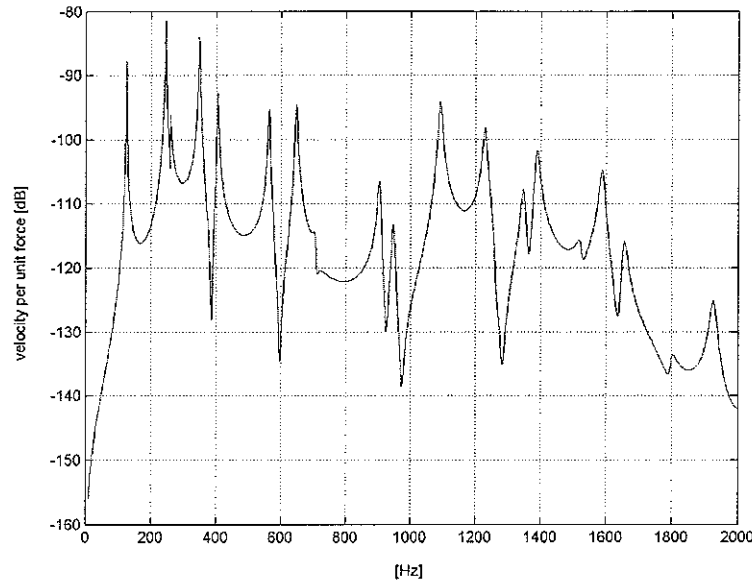


Figure (5): 0-2000 Hz plot of mobility between the chosen e/o points.

The plots show many modes of vibration in the frequency range of interest. Each mode involves generally in-plane and out-of-plane motion in all 3 plates. The proportion of energy in each plate, considering in-plane and out-of-plane motion, varies from mode to mode. This results variations of the general amplitude of the frequency average mobility. Some modes are characterized by large amount of energy in one plate only, e.g. bending substantially of only one plate. Other modes involve motion of two or more plates.

A brief description of the mode shapes that characterize the dynamic of the model is presented. The first modes of the structure correspond to the bending modes of the two larger plates. The nodal displacements are in the same direction as that of the excitation force. In Figure (6) is shown the first mode of the structure, which is at 128 Hz. This mode is predominantly the first bending in the zx plane of the second plate.

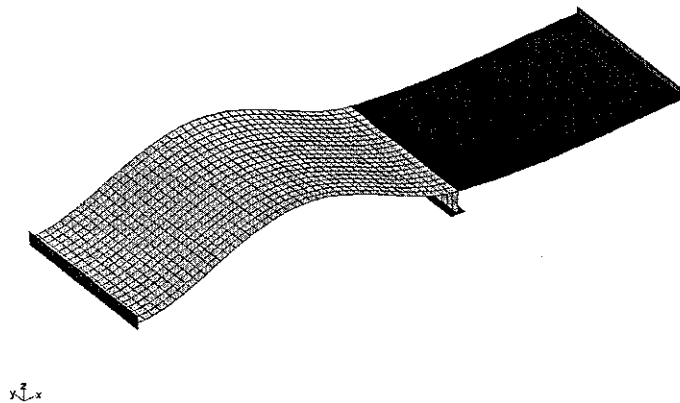


Figure (6): mode 1 at 128 Hz, mainly the first bending of the second plate in the zx plane.

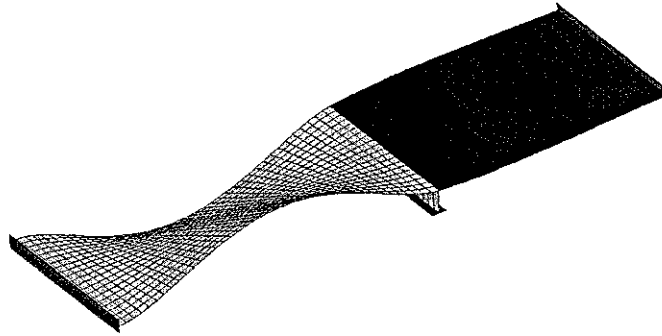


Figure (7): mode 2 at 210 Hz, mainly the first bending of the second plate in the zy plane.

The second mode is at 210 Hz. This mode is predominantly the first bending in the zy plane of the second plate. At higher frequency bending modes of the first plate can be observed. Figure (8) shows the third mode of the structure. Its natural frequency is at 246 Hz and is the mainly first bending in the zx plane of the first plate. As the frequency increases the structure shows several mode of vibration that involves mainly the deformation of the first or the second plate. Some mode shapes, such as the one shown in Figure (9), involves significant deformation of the third plate, i.e. the joint, in an indirect way. The motion of the third plate is mainly driven by the deformation of the first and the second plate, which show in Figure (8) their third and second bending in the zx plane respectively.

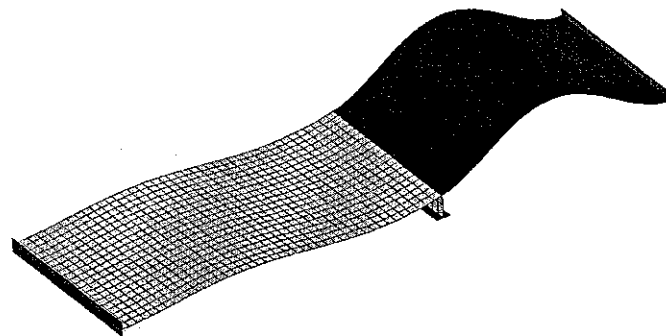


Figure (8): mode 3 at 246 Hz, mainly the first bending of the first plate in the zx plane.



Figure (9): mode 7 at 650 Hz, the motion of the third plate is mainly driven by the deflection of the two other plates.

The mode of vibration shown in Figure (10) has a natural frequency of 1232 Hz and it is the lowest mode that has substantial bending of the third plate. This mode of vibration is of interest since it is likely to result in a high level of variability in the FRFs, when uncertainties are introduced in the joint properties.

In Figure (4) low amplitudes of mobility can be seen in the 1600-2800 Hz band and in the 4000-5500 Hz band. In both bands are involved modes of vibration of the type shown in Figures (11) and (12) respectively. These are mainly in-plane modes of vibration for the complete structure, for which the displacements in the z direction are negligible if compared to the displacements in the xy plane. Therefore due to our choice of excitation/observation points, these modes are either weakly excited or respond weakly.

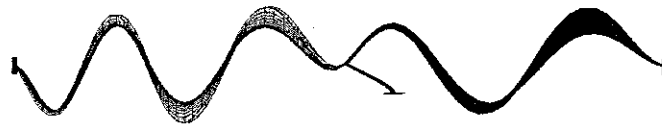


Figure (10): mode 17 at 1232 Hz, lowest mode that has substantial bending in the third plate.

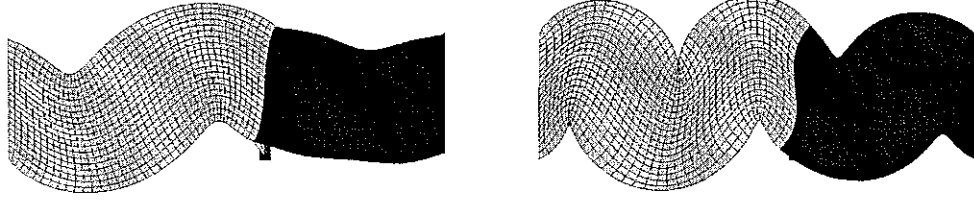


Figure (11): mode 24 and 42 at 1644 Hz and 2740 Hz respectively. Mainly the 4th and 6th in-plane symmetric motion of the structure respectively

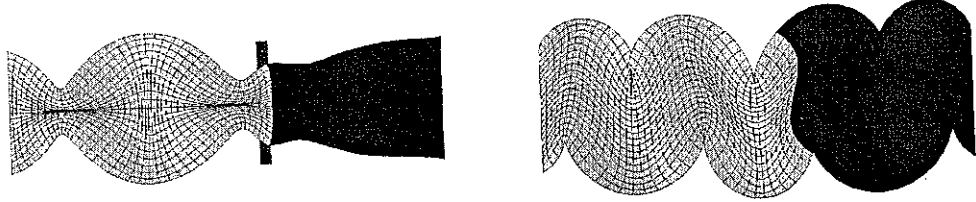


Figure (12): mode 72 and 73 at 4038 Hz and 4047 Hz respectively. Mainly the 5th and 8th in-plane anti-symmetric and symmetric motion of the structure respectively.

Figure (4) shows also the typical transition from low frequency to high frequency behaviour as the frequency and the modal overlap increases. At low frequency there are distinct resonant peaks. As the frequency increases, the peaks become less distinguishable. The half-power bandwidth of a mode (response within 3 dB of the peak) becomes comparable with the resonant frequency spacing. The half-power bandwidth is given by

$$\Delta f = \eta(f) f_n \quad (3.1)$$

where $\eta(f)$ and f_n are the loss factor and the resonance frequency respectively. For our structure the loss factor is assumed independent of frequency. The half-power bandwidth is therefore a function of frequency. Thus as f_n increases, so does Δf . At high frequencies, the modes overlap, i.e. a resonance peak lies within the bandwidth of its neighbourhoods and individual resonances can no longer be distinguished from one another. This can be quantified by the modal overlap factor M , which is defined as

$$M = \eta(f) n(f) f \quad (3.2)$$

where $n(f)$ is the modal density. The modal density is defined as the expected number of modes per unit frequency. The modal density is an asymptotic value and can be defined strictly only for frequency bands characterized by a sufficient number of modes. It is an

extensive parameter and is independent of the boundary conditions. For a plate in bending the flexural waves predominantly contributes to the number of modes in a given band. The modal density then takes the form

$$n(f) = \frac{A}{2} \sqrt{\frac{12\rho(1-\nu^2)}{Eh^2}} \quad (3.3)$$

where A is the area, E, ρ and ν the material properties and h the thickness of the plate. Equation 3.3 shows that for a plate in bending $n(f)$ is independent of frequency.

If we take into account for each plate of the structure only the bending modes, then the modal density of the whole structure will have the same expression of 3.3 with A given by the sum of the surface areas of the three plates. We obtain $n(f) = 0.0082$ which are roughly 8 modes per kHz.

The loss factor and the modal density are independent of frequency, the modal overlap factor becomes therefore a linear function of frequency, as shown in Figure (13).

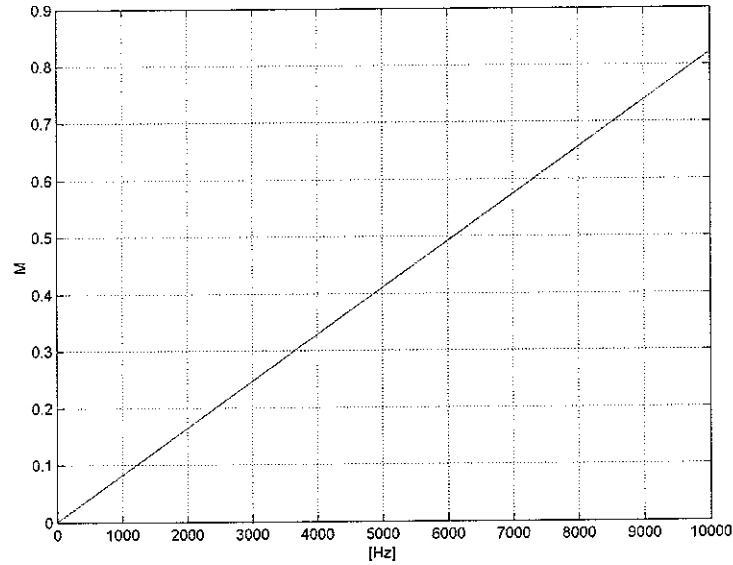


Figure (13): modal overlap factor M .

Using equation (3.1) we can conveniently rewrite equation (3.2) as

$$M = \frac{\Delta f}{1/n(f)} \quad (3.3)$$

where $1/n(f)$ is the average spacing between natural frequencies. We can therefore distinguish zones in frequency characterised by high values and low values of the modal overlap factor:

$M \ll 1$	low modal overlap factor
$M \gg 1$	high modal overlap factor

Mid-frequency is typically characterized by $M \approx 1$.

From Figures (4) and (13), we can see that below 5000 Hz the structure response is characterised by a low modal overlap factor, while above the structure vibrates mainly in a mid-frequency manner.

The sensitivity of a structure to uncertainties is generally a function of frequency, i.e. variability in the structure's response tends to increase with frequency. Peaks can be indistinguishable even in frequency ranges characterised by low modal overlap factor. The definition of a stochastic modal overlap factor describes this phenomenon, as will be shown in chapter 5.

3.3. CMS-Finite Element Analysis

In this section the same problem is analysed using CMS-FEA. The complete structure is divided into three substructures and one coupling interface. A CMS fixed-interface method has been preferred for its simplicity of implementation. Three separate local analyses, one for each substructure, are performed. For each substructure a certain number of component modes is retained, as listed below:

- first plate: 150 fixed-interface normal modes, up to 25000 Hz
96 constraint modes
- second plate: 200 fixed-interface normal modes, up to 30000 Hz
96 constraint modes
- third plate: 50 fixed-interface normal modes, up to 32000 Hz
96 constraint modes

For all three plates the same number of constraint modes is retained, corresponding to the dimension of the vector of the coupling degrees of freedom. At this stage no reduction technique is applied to the vector of coupling degrees of freedom. The reduction in the order of the complete structure will only be due to the reduction of the vector of the interior degrees of freedom.

Once the transformation matrix $[\psi]$ for each substructure is established, and the global matrices of the reduced order system assembled, the reduced order eigenproblem is solved. The CMS-FEA took 180 seconds to run, almost 60% less than the full finite element analysis. The order of the model was reduced from 11088 for full FE to 688 for the CMS model. In Figure (14) a comparison between the mobility computed by the full FEA and the CMS-FEA is presented.

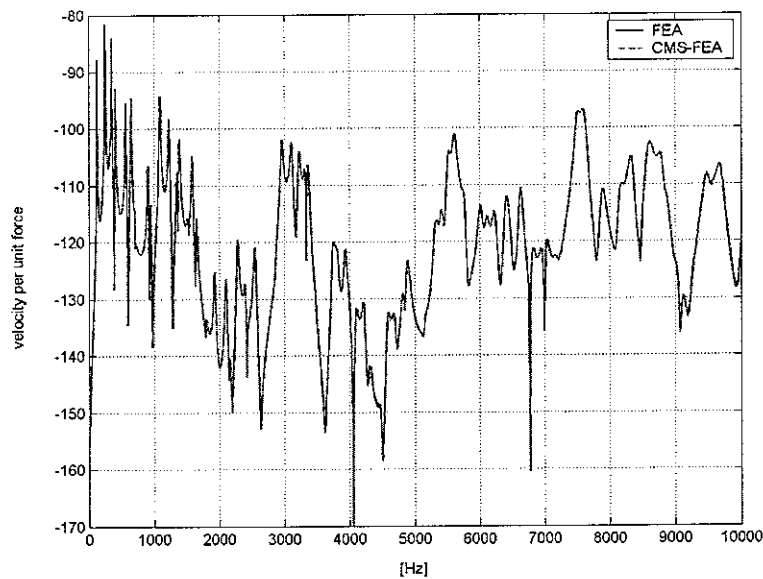


Figure (14): mobility computed by the full FEA and the CMS-FEA.

Almost exactly the same response is predicted, apart from some small variations in the higher modes due mainly to the number of fixed-interface normal modes retained for each plate and some differences at lower frequencies due mainly to small residual effects in the coupling. In Figure (15), a comparison of the natural frequencies is presented. Good agreement is found up to 10000 Hz

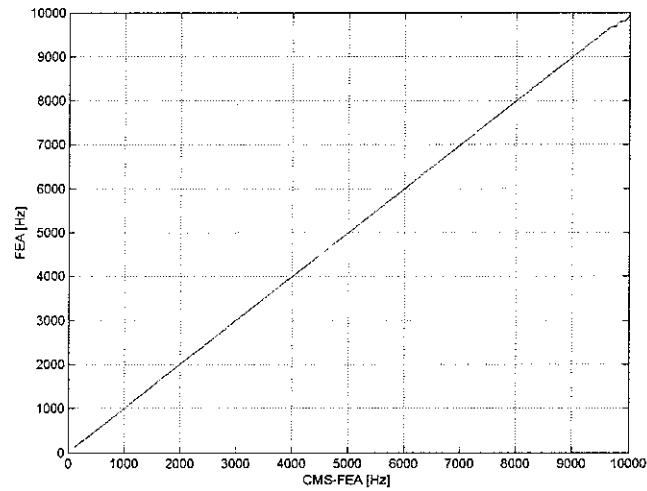


Figure (15): natural frequencies computed by the full FEA and the CMS-FEA.

In the following sections uncertainties and variability will be introduced in the structure. The advantages of using CMS-FEA for the evaluation of the response statistics are then seen. A substantial reduction in computing time will be found, when long Monte Carlo simulations are needed for the evaluation of the response statistics. The statistics obtained by the full FEA and the CMS-FEA agree very well.

4. Uncertainty and Variability

Uncertainty and variability in the properties of a structure, such as its mass, stiffness and dimensions, arise from a number of causes, and are characterized by the sensitivity of the response of the structure to typical variation in its properties.

A first source of uncertainty is related to the fact that typical design models are assumed to be robust for the entire manufactured ensemble of structures. Manufacturing variations and tolerances, dimensions, the properties of joints and welds etc. and the material properties such as density and elastic modulus, typically differ from one item to the next. Measurements taken on a set of nominally identical structure in general show an amount of variability, e.g. the same modes of vibration are found at slightly different frequencies. The amount of variability generally increases with frequency.

A second source of variability is due to the fact that the properties of a single structure might vary with time due to environmental effects (such as changing temperature), ageing, wear and changes in operating conditions (e.g. load, orientation). Measurements taken on a single structure at different times, i.e. under different weather conditions, humidity, temperature etc., will in general give different values for the measured responses; again the amount of variability increases with frequency.

On the other hand, the variability of measurements will result in a level of uncertainty in the exact values of the properties to use in a numerical model. Thus the predictions of a numerical model will generally differ from the actual behaviour of the structure. As a result, the parameters in a numerical model differ from those of the actual structure, and the parameters of the actual structure will in general be different to those of other nominally identical structures.

It becomes therefore of practical interest, to predict not only the ‘baseline’ response, but also to estimate the statistics or spread of the responses of different realisations of the structure, which are more representative of the ensemble behaviour.

Uncertainties can be quantified in a numerical model in different ways. One possibility is in terms of physical properties of a structure, i.e. geometric properties (length, thickness etc), material properties (density, elastic modulus, stiffness etc.) and the properties of joints (weld positions, stiffness etc). These variables are then used to define mass and stiffness matrices in a FE model. The physical properties are continuous random fields defined over the whole structure or substructure, and consequently there are spatial correlations and cross-correlations (e.g. spatial correlation in the thickness of a plate). This results in difficulties in including the uncertainties in the numerical model, e.g. how these correlations can in practice be measured.

Alternatively, uncertainty can be defined in terms of the modal properties of a structure, for example its natural frequencies. The natural frequencies are discrete, and there are relatively few in a given frequency range. Furthermore, they are relatively easy to measure. It should be noted that the physical and modal properties are uniquely related. The modes are uniquely defined once the physical properties are known, and they can be found numerically from the physical properties by modal analysis.

A number of statistical approaches have been developed to allow for uncertainties in the parameters of a structure to be included in a numerical analysis. The amount of variability, i.e. the sensitivity of the structure's response to uncertainties, is generally related to the frequency range of interest. At low frequency a single deterministic FEA is generally ok to describe the behaviour of a structure. At high-frequency, as the response gets more sensitive to uncertainties, statistical approaches such as statistical energy analysis (SEA) [1], which assumes wide random variations in the properties of the structures, are suitable. In the mid-frequency range, which is the subject of this paper, a statistical approach is required, but the properties do not vary as widely as assumed in SEA.

Parameter uncertainties can be incorporated in deterministic models in several ways [2]. Monte Carlo simulations are generally used to find the response statistics, by repeating an exact calculation many times with different sets of parameters. Stochastic FE methods [7,8] can be used, where the continuous physical properties of the structure vary statistically and are meshed in a manner analogous to that used to discretise the structure itself. A possible alternative is by finding perturbational relations between parameters and response quantities [3,4,5,6].

At mid-frequency the characteristic wavelengths of interest are such that large FE models are generally needed for modelling even a single realisation of a structure. In addition the variability in the structure's response due to uncertainties becomes significant in this frequency range. Repeating the solution procedure for the evaluation of the structure's response statistics as in a Monte Carlo simulation becomes unfeasible. Reducing the order of the model becomes a major task and CMS [9] can achieve this. Furthermore the uncertainties are introduced locally rather than globally in the structure. Even using CMS this is still a computationally expensive task, and hence there is a need to develop methods to substantially reduce computational cost.

A local modal/perturbational method [3,4,5,6] is presented in chapter 6. This method encompasses both the advantages deriving from the use of a sub-structuring technique and the use of a perturbational approach. This method adopts a fixed interface/constraint mode model and a local perturbation to estimate frequency response functions and their statistics. The statistics follow from the perturbation at an insignificant cost. All the methods discussed above are generally employed when the degrees of uncertainty is low. For larger degrees of uncertainty alternative approaches are then required.

5. A Numerical Example: Uncertain Properties

5.1. Model Description

The numerical model considered in this section is the same as that presented in chapter 3. In the previous chapter the numerical model was deterministic. In this section uncertainties are introduced in the structure and the interest is turned on the response statistics rather than the response of a single realisation of the structure. When variability is considered a single realisation of the structure is not representative of the behaviour of the ensemble. Therefore there is the need to evaluate statistics of the ensemble, i.e. mean value, percentiles, standard deviation, etc.

For large FE models a sub-structuring technique, such as CMS, is generally suitable even for a single deterministic realisation of the structure. When statistics of the response are of interest, using a sub-structuring technique is almost mandatory. Evaluation of the response statistics via a Monte Carlo simulation is a costly prohibitively procedure; several advantages of using CMS fixed-interface method are shown below.

The aim of this report is to analyse the behaviour of structures with uncertain joint properties. Therefore uncertainties are introduced in the properties of the third plate, which represents the structure's joint. Uncertainties can be introduced in several ways in the properties of a structure, mainly in its physical properties or in its modal properties. The two are obviously related. The latter are easy to measure quantities, while the former typically present the problem of the definition of a set of joint probability functions. At this stage of the research only uncertainties in the physical properties of the joint are considered.

In the numerical example the Young's modulus E of the joint is considered uncertain. Its variability is defined by a one dimensional probability density function (pdf). At this stage for simplicity no joint-pdfs are introduced, e.g. the way in which uncertainties in E are correlated with uncertainties in the thickness, length, etc. As E is related to the stiffness of the joint, uncertainties in E will result in uncertainties in the joint stiffness. Changes in the structure's eigenfrequencies should be observed.

In this section the pdf of E is assumed to be Gaussian with mean E_0 and standard deviation σ_E given by

$$E_0 = 210 \text{ [GPa]}$$

$$\sigma_E = 0.1 * E_0$$

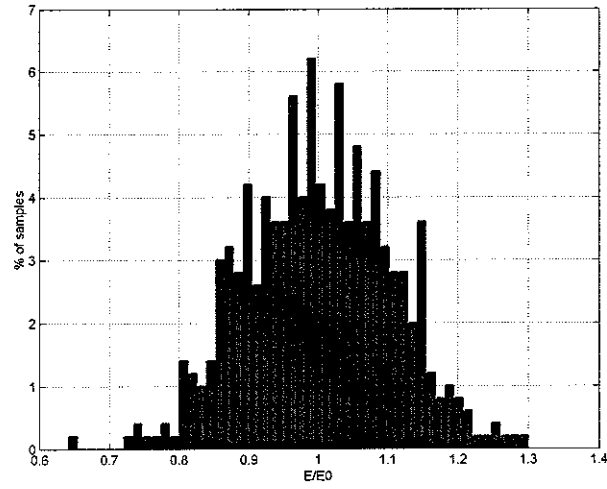


Figure (16): distribution of E/E_0 .

A Monte Carlo simulation with 200 members is performed. Figure (16) shows the actual numerical distribution of E in this simulation. The plot is centred over the assigned baseline value E_0 .

96% of the realisations lie within the $2\sigma_E$ of the mean. In theory negative values of E might occur: in practice, with $\sigma_E = 0.1 * E_0$, these are extremely rare and did not occur in the Monte Carlo simulation. It would also be interesting to test the goodness-of-fit of the numerical data compared to an assumed probability distribution, i.e. normal.

5.2. Monte Carlo Simulation

In this section a Monte Carlo simulation is performed to evaluate the response statistics. For each sample of the distribution of E , the numerical model is solved. In the full FEA the large eigenproblem of the complete structure is re-solved each time. In the CMS-FEA the large eigenproblem is divided into smaller eigenproblems. The re-analysis only involves the substructures in which the uncertainties are introduced together with the assembled, global eigenproblem, which is of very small order compared to full FEA.

The type and the number of component modes retained in the CMS-FEA are the same as these chosen in section 2.3. The baseline mobility is presented in chapter 3, consisting of 300 modes up to 16000 Hz. Results for the mobility are shown up to 10000 Hz and the frequency resolution is 1 Hz.

The full FEA took almost 34 hours to run (on a *Pentium 4, 1.7GHz*). The CMS-FEA took almost 7 hours to run (on a *Pentium 4, 1.7GHz*), almost 80% less than the time need to solve the full FEA.

In Figures (17) and (18) plots of mobility obtained from 200 Monte Carlo simulation are presented. The former is obtained with a full FEA while the latter with a CMS-FEA. The variability shown for both analysis methods seems to be the same over the frequency band of interest. In both pictures can be observed how the uncertainty in the joints is influencing the structure response. At low frequency the variability is generally small, beside a certain amount in the system's static response. As the frequency increase the amount of variability in the response tends to increase and at higher frequency tends to be larger such that the shifting in the natural frequencies is comparable with the average spacing between natural frequencies.

In Figures (19) and (20) for completeness the plots of mobility are shown on a logarithmic scale. Large variability can be observed around 1200 Hz, in a relative low-frequency band. As we have seen in chapter 3, at this frequency the structure shows mainly the bending of the third plates in the zx plane. One such mode is at 1232 Hz and is shown again in Figure (21). The uncertainties in the joint here have great influence on the response of the structure.

If we compare Figures (17) or (18) and (4) which shows the baseline value of the structure's response, we note that despite a relatively low value of the modal overlap factor, individual resonance peaks start to be less distinguishable from around 3000 Hz. The reason for this is the relative importance of variability with respect to the frequency spacing. This phenomenon can be explained if a stochastic modal overlap factor is introduced.

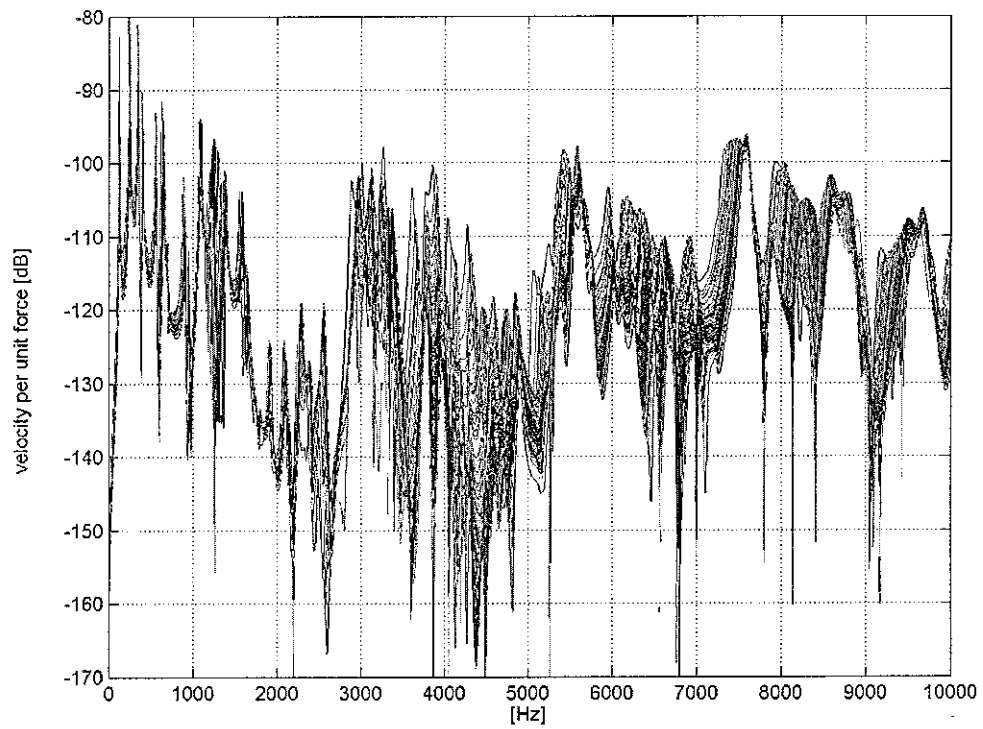


Figure (17): realisations from FEA. 200 Monte Carlo simulation.

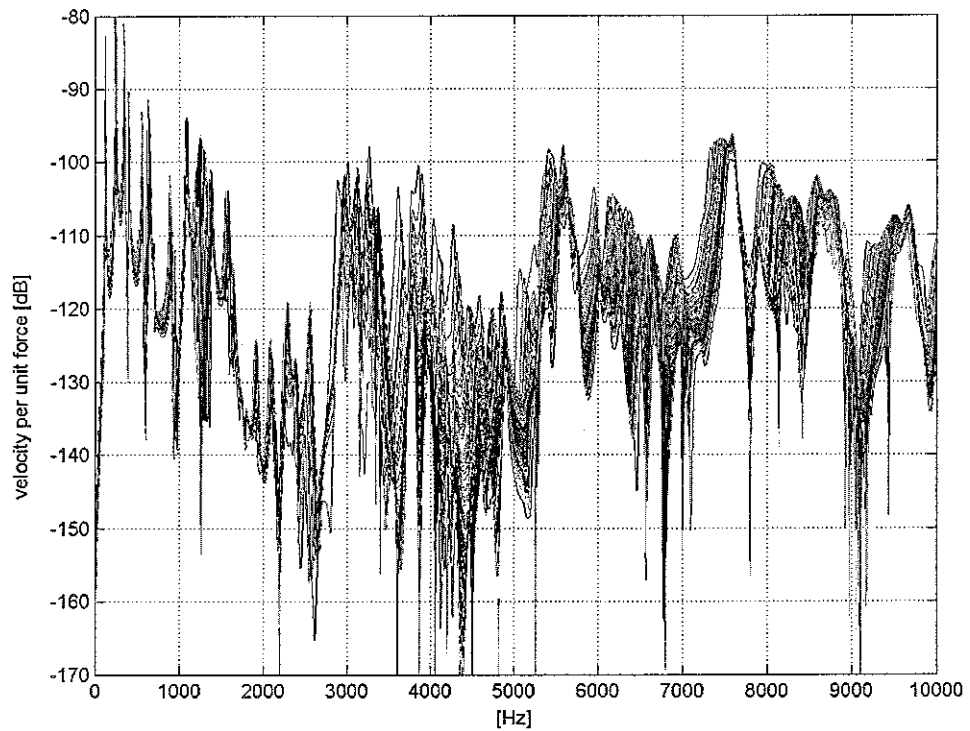


Figure (18): realisations from CMS-FEA. 200 Monte Carlo simulation.

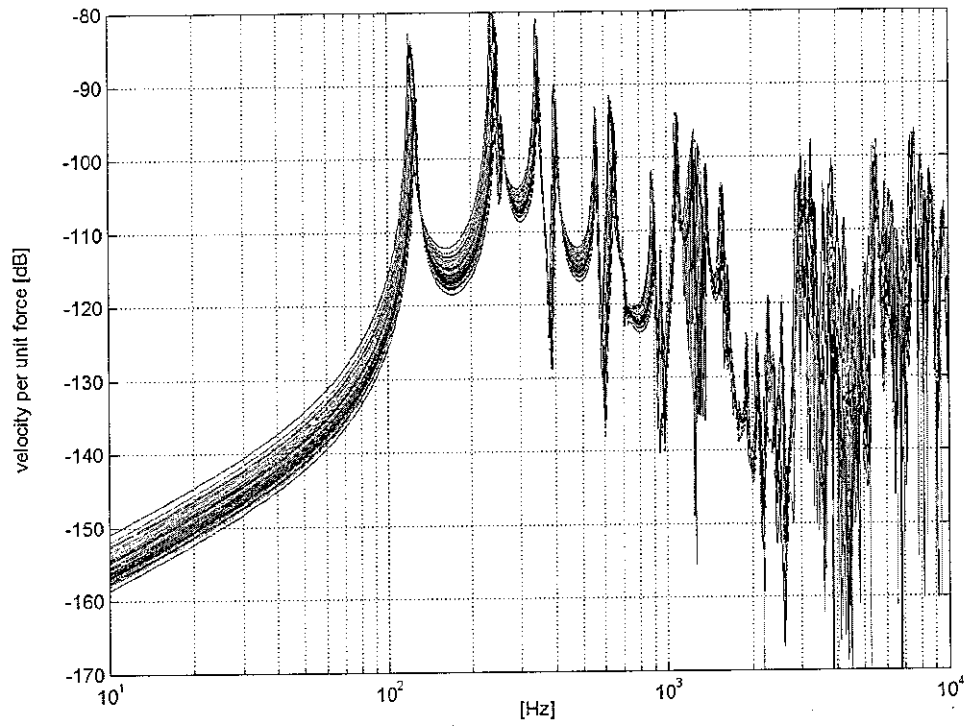


Figure (19): realisations from FEA. 200 Monte Carlo simulation.

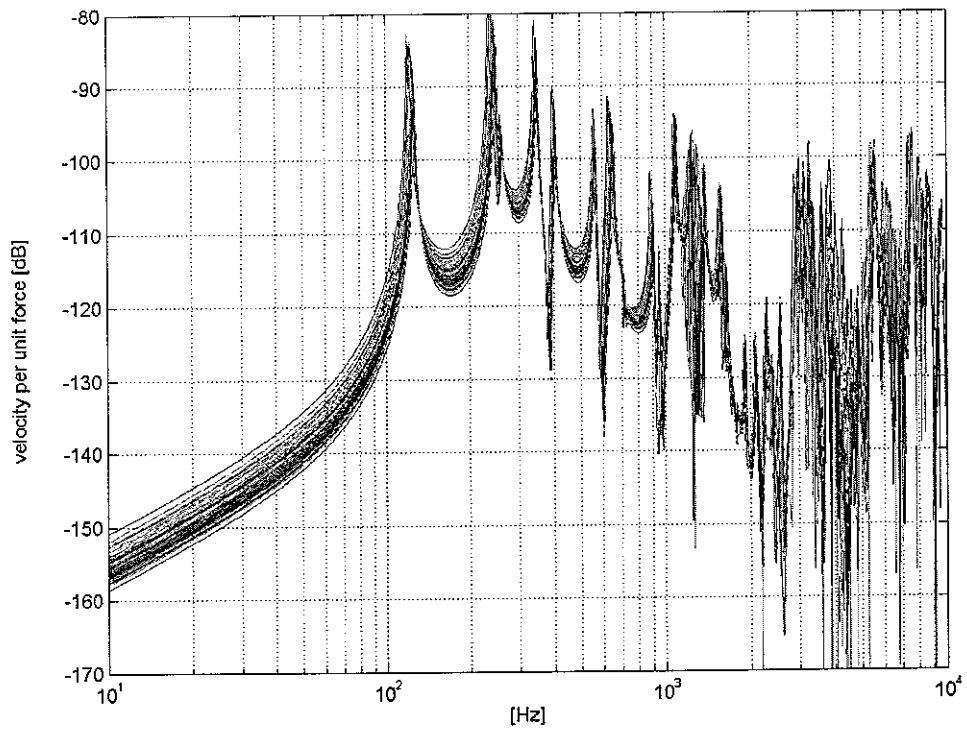


Figure (20): realisations from CMS-FEA. 200 Monte Carlo simulation.



Figure (21): mode 17 at 1232 Hz, lowest mode that has substantial bending in the third plate.

The stochastic overlap S can be defined as the ratio of the standard deviation of the natural frequencies, i.e. the shifting of the natural frequencies due to variability in the structure response, and the resonant frequency spacing. The stochastic modal overlap factor can be expressed as

$$S \approx \frac{2\sigma_{\omega_n}}{1/n(\omega)} \quad (5.1)$$

where σ_{ω_n} is the standard deviation, on average, of the natural frequencies. Since typically $\omega_n \propto \sqrt{E}$, then

$$\sigma_{\omega_n} \propto \frac{1}{2} \sigma_E \omega_n \quad (5.2)$$

where σ_E is the standard deviation of the joint's modulus E . Equation (5.1) can be rewritten as

$$S \approx \frac{\sigma_E \omega}{1/n(\omega)} = \frac{\sigma_E f}{1/n(f)} \quad (5.3)$$

As the modal density is constant, S and M becomes a function of frequency only. In Figure (22) are compared. The figure shows that the stochastic modal overlap factor becomes greater than unity before the modal overlap factor. The spread in the structure's responses becomes comparable to the resonant frequency spacing. The mean response of the ensemble will tend not to show distinct resonance peaks in frequencies zones where the response of an individual member will in generally. This is evident in figure (23).

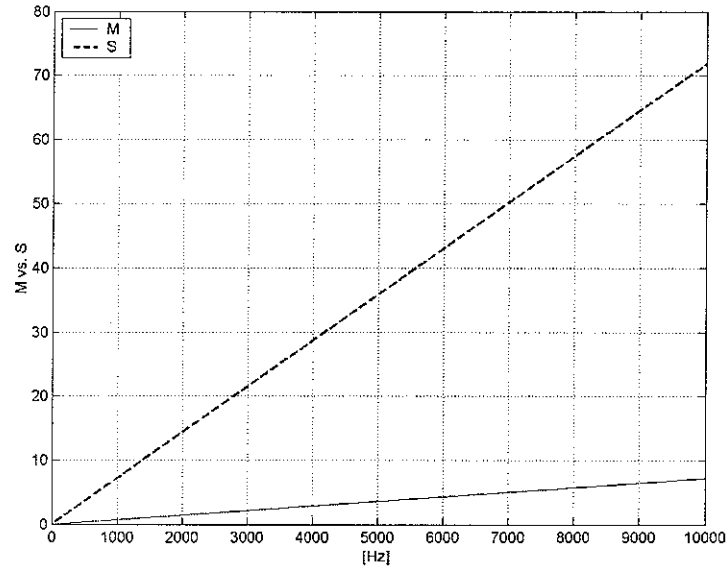


Figure (22): modal overlap factor vs. stochastic overlap factor.

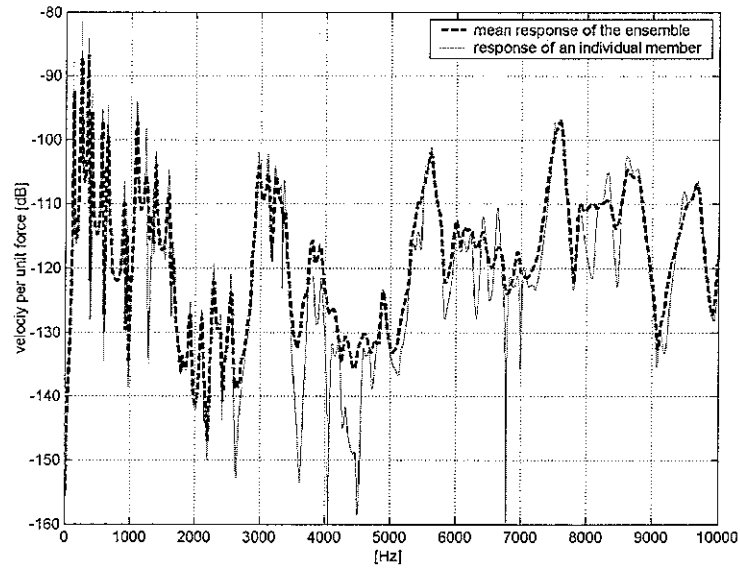


Figure (23): mean response of the ensemble vs. response of an individual member.

It should be noted that equation 5.2 is not exact since only E of the joint changes while the natural frequencies of the structure depend also on the first and the second plate. Quantifying the contribution of the joint stiffness to σ_{ω_n} , i.e. to the potential energy in each mode, might be also interesting.

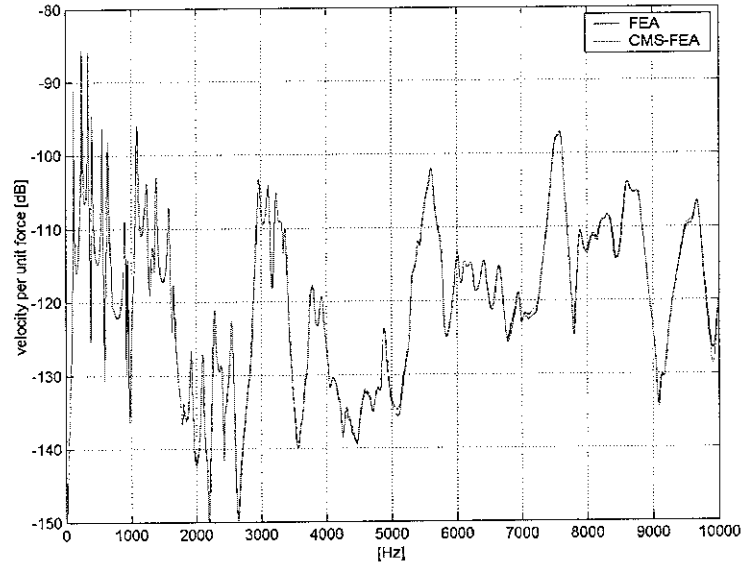


Figure (24): mean values, FEA vs. CMS-FEA.

Figures (24), (25), (26) and (27) show some response statistics. The mean values, normalised standard deviation and 50% percentiles of the ensemble estimated by full FEA and CMS-FEA show good agreement over the frequency range of interest.

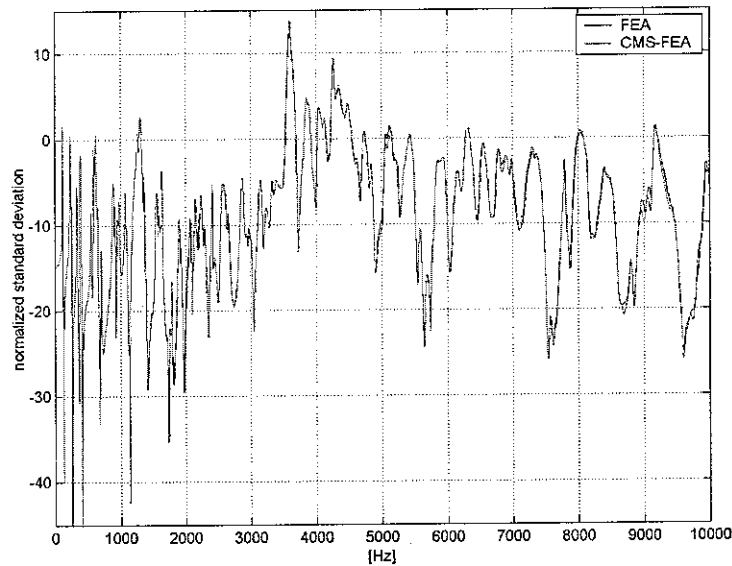


Figure (25): normalised standard deviation, FEA vs. CMS-FEA.

The standard deviation is normalised with respect to the square of the mean value. Values around +10 dB are shown around 4000 Hz, which reflect the large amount of variability in the same band observed in Figures (17) and (18). It would be interesting to see the shape of the distribution of each peak above its mean value, i.e. a direct measure of the spread of the response. Future work will concern the relations between all the standard deviations of

interest. Statistics such as 90% percentiles and min/max values might also be of interest, those would require, to better estimate the tails of the distribution, a substantial larger number of Monte Carlo simulations.

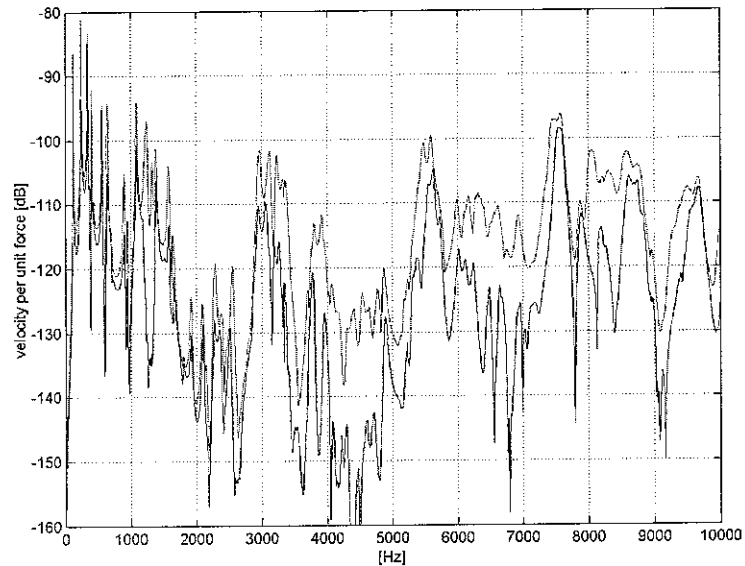


Figure (26): 50% percentiles, FEA.

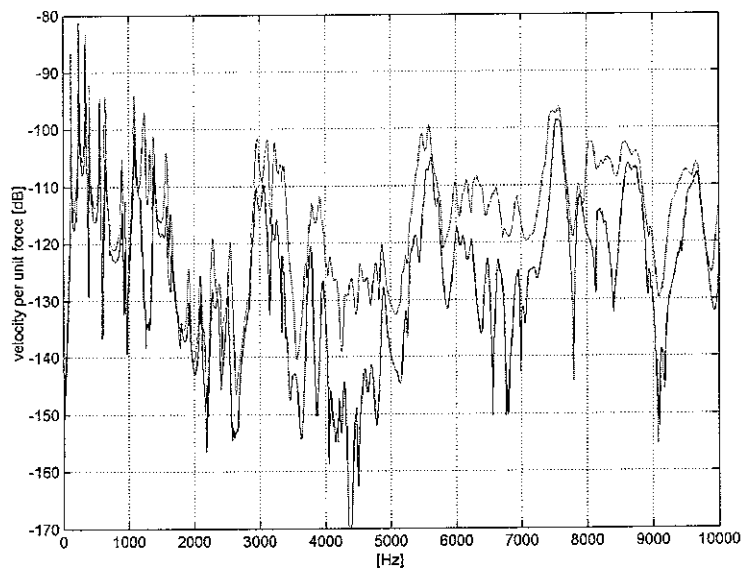


Figure (27): 50% percentiles, CMS-FEA.

The advantages of using a CMS-FEA are clear. The reduction in the computing time is substantial while the results achieved generally retain high accuracy. However, a direct Monte Carlo simulation is still a computationally expensive task. In the next chapter an alternative method is introduced which will allow the evaluation of the statistics at a much cheaper cost.

6. Future Work: Perturbational Methods

Estimating the response statistics via a direct Monte Carlo simulation is generally a computationally expensive task. As seen in the previous chapters, when the structure is likely to be divided in substructures and uncertainties introduced locally in each substructure then, rather than full FEA, the use of CMS-FEA in the evaluation of the response statistics already results in a substantial reduction in the computing time. However, to define the probability levels at the tails of the distributions a large amount of numerical computation is needed such that a direct Monte Carlo simulation is often impractical. One alternative involves perturbational methods [3,4,5,6], leading to combined perturbational Monte Carlo simulations.

Perturbational methods in essence use a Taylor series expansion to relate perturbations in properties of a structure to perturbations in the modal properties. The Taylor series is often truncated after the first few terms and an assumption is made that the function relating the perturbations in the properties of the structure to the perturbations in the response can be approximated by a low order polynomial.

In order to calculate a Taylor series expansion for the dynamic properties of a structure, it is necessary to calculate the derivatives of the global modal properties with respect to a number of design variables. As in [3], the derivatives of the eigenvalues are given by

$$\frac{\partial \lambda_i}{\partial \delta_j} = \phi_i^T \left[\frac{\partial K}{\partial \delta_j} - \lambda_i \frac{\partial M}{\partial \delta_j} \right] \phi_i \quad (6.1)$$

where λ_i and ϕ_i are the i^{th} unperturbed eigenvalue and eigenvector and δ_j the j^{th} design variable. To estimate the eigenvector derivatives several ways are possible. In general the eigenvector derivatives can be expressed in terms of a linear combination of the unperturbed eigenvectors. The eigenvector derivatives are then given by

$$\frac{\partial \phi_i}{\partial \delta_j} = \sum_p a_{ip} \phi_p \quad (6.2)$$

where the index p runs over the global modes and where

$$a_{mn} = \frac{\phi_n^T \left[\frac{\partial K}{\partial \delta_j} - \lambda_m \frac{\partial M}{\partial \delta_j} \right] \phi_m}{(\lambda_m - \lambda_n)} \quad \text{if } m \neq n \quad (6.3)$$

$$a_{mm} = -\frac{1}{2} \phi_m^T \left[\frac{\partial M}{\partial \delta_j} \right] \phi_m \quad \text{if } m = n \quad (6.4)$$

The use of perturbational methods in Monte Carlo simulations is particularly advantageous when the uncertainties are defined via an ensemble of dynamic properties. In the numerical example presented in chapter 5, the uncertainties were introduced locally in the structure via an ensemble of physical properties. Only the Young's modulus of the joint was considered uncertain and a one dimensional probability density function was assigned. Since E is related to the stiffness matrix K , we can say that approximately, the variation in one parameter is proportional to variation in the other so that

$$\partial E \propto \partial K \quad (6.5)$$

while the mass matrix remains unperturbed. The perturbational equations 6.1 and 6.2 will then simplify as

$$\frac{\partial \lambda_i}{\partial \delta_j} = \phi_i^T \left[\frac{\partial K}{\partial \delta_j} \right] \phi_i \quad (6.6)$$

and

$$\frac{\partial \phi_i}{\partial \delta_j} = \sum_p a_{ip} \phi_p \quad (6.7)$$

where

$$a_{mn} = \frac{\phi_n^T \left[\frac{\partial K}{\partial \delta_j} \right] \phi_m}{(\lambda_m - \lambda_n)} \quad \text{if } m \neq n \quad (6.8)$$

$$a_{mm} = 0 \quad \text{if } m = n \quad (6.9)$$

Nevertheless, a realistic representation of the joint uncertainties would require in general a statistical description of all the joint properties including the definition of several joint probability functions, which makes this way of approaching the problem difficult to implement and impractical. Defining an ensemble in terms of the dynamic properties of a structure is suitable for many reasons. If the ensemble is defined in terms of the statistics of the natural frequencies of a structure, then the comparison with experimental measurement is straightforward.

Future work will concern the definition of a dynamic ensemble for the structure's joints. Perturbational Monte Carlo simulations will be computationally much cheaper while retaining accuracy in the results.

In [3,4,5,6], a local modal perturbational method is considered. The idea is to take advantages of both a CMS approach and a perturbational approach. In the first step the structure is divided in substructures and the order of the model is reduced. Uncertainties are then introduced locally in a substructure, defining an ensemble in terms of the dynamic properties of the substructure, i.e. in its local modal properties. A perturbational relation is then found between perturbation in local modal properties and perturbation in the global modal properties of the structure. A local modal perturbational Monte Carlo simulation is then used to find the response statistics, generally at an insignificant cost.

The definition of an ensemble in terms of dynamic properties for the structure's joints and the implementation of a local modal Perturbational Monte Carlo simulation are the long-term aim of this research.

7. Concluding Remarks

This report concerned a number of issues involved in the evaluation of the response of uncertain complex built-up structures, particularly when there is uncertainty in the properties of joints

To address the problem of large FE models, typical of mid-frequency analyses, a substructuring technique, CMS, was introduced. In chapter 3 a full FEA and a CMS-FEA were compared on a numerical model. Good agreement was found in the frequency range of interest while the structure's response was found by the CMS-FEA at a cheaper cost.

In chapter 5 uncertainties were introduced in the numerical model. The advantages of using CMS, when direct Monte Carlo simulation is used to evaluate the statistics of the response and when the uncertainties are localized in a single substructure, were shown.

Furthermore, in chapter 6 some guidelines were given for future work, concerning the use of perturbational methods to evaluate the system's response to avoid long computer runs, which are typical of direct Monte Carlo simulations.

8. Acknowledgements

The work carried out for this research is within the "European Doctorate in Sound and Vibration Studies" which is supported through a European Community Marie Curie Fellowship.

I am grateful to all ISVR members, and in particular my supervisor Dr. Brian Mace, for the support and encouragement during my stay in Southampton.

I would also like to thank KUL since this research is part of the Belgian program on Interuniversity Poles of attraction initiated by the Belgian State, Prime Minister's Office, Science Policy Programming.

9. References

- [1] Courtney B. Burroughs, Raymond W. Fischer, Fred R. Kern, *An introduction to statistical energy analysis*, J. Acoust. Soc. Am., 101 (4), April 1997, pp. 1779-1789.
- [2] R. S. Langley, *The Dynamic Analysis of Uncertain Structures*, Structural Dynamics Recent Advances, Proceedings of the 7th International Conference, Invited Paper.
- [3] B. R. Mace, P. J. Shorter, *A Local Modal/Perturbational Method for Estimating Frequency Response Statistics of Built-Up Structures with Uncertain Properties*, Journal of Sound and Vibration, vol. 242, no.5, 2001, pp.793-811.
- [4] MACE, B R. *Estimation of frequency response statistics in structures with uncertain parameters*, ISMA 25, 25th International Conference on Noise and Vibration Engineering, Leuven, 2000..
- [5] Brian Mace, *Mid-frequency Vibration Analysis and Application to a Two-Rod System*, Structural Dynamics Recent Advances, Proceedings of the 7th International Conference.
- [6] P. J. Shorter, 1998 Ph.D. Thesis. University of Auckland, New Zealand. *Combining Finite element and Statistical Energy Analysis*.
- [7] Armen Der Kiureghian and Jyh-Bin Ke, *The stochastic finite element method in structural reliability*, Probabilistic Engineering Mechanics, 1988, Vol. 3, No. 2, pp. 83-91.
- [8] H Benaroya and M Rehak, *Finite element methods in probabilistic structural analysis: A selective review*, Appl. Mech. Rev., Vol. 41, No. 5, May 1988, pp. 201-213.
- [9] R. R. Craig, Jr., *Substructure Methods in Vibration*, Transaction of the ASME, vol. 117, Special 50th Anniversary Design Issue, June 1995, pp. 207-213.
- [10] Andrew M. Brown and Aldo A. Ferri, *Application of the Probabilistic Dynamic Synthesis Method to Realistic Structures*, AIAA Journal, Vol. 37, No. 10, October 1999, pp. 1292-1297.
- [11] Gladwell, G. M. L., *Branch Mode Analysis of Vibrating Systems*, Journal of Sound and Vibration, Vol.1 , No. 1, 1964, pp. 41-59.
- [12] Hurty, W. C., *Dynamic Analysis of Structural Systems Using Component Modes*, AIAA Journal, Vol. 3, No. 4, 1965, pp. 678-685.
- [13] Craig, R. R., and Bampton, M. C. C., *Coupling of Substructures for Dynamic Analysis*, AIAA Journal, Vol. 6, No. 7, 1968, pp. 1313-1319.

- [14] Goldman, R. L., *Vibration Analysis by Dynamic Partitioning*, AIAA Journal, Vol. 7, No. 6, 1969, pp. 1152-1154.
- [15] Hou, S. N., *Review of Modal synthesis Technique and a New Approach*, Shock and vibration Bulletin, Bulletin 40, Pt. 4, 1969, pp. 25-30.
- [16] Bajan, R. L., Feng, C. C., and Jaszlics, I. J., *Vibration Analysis of Complex Structural Systems by Modal Substitution*, Shock and Vibration Bulletin, Bulletin 39, Pt. 3, 1969, pp. 99-105.
- [17] MacNeal, R. H., A Hybrid Method of Component Mode Synthesis, Computers and Structures, Vol. 1, No. 4, 1971, pp. 581-601.
- [18] Benfield, W. A., and Hrudá, R. F., Vibration Analysis of Structures by Component Mode Substitution, AIAA Journal, Vol. 9, No. 7, 1971, pp. 1255-1261.
- [19] R.R. Craig, Jr., *A Review of Time-domain and Frequency-Domain Component Mode Synthesis Methods*, The International Journal of Analytical and Experimental Modal Analysis, vol. 2, no. 2, April 1987, pp. 59-72.
- [20] Noor, A. K., and Petrs, J. M., Reduced Basis Technique for Nonlinear Analysis if Structures, AIAA Journal, Vol. 18, No. 4, 1980, pp. 455-462.